Davidson[22] has described how continuum opacities limit the spectroscopic excursions of these stars during outburst. The Nova Cas 1993 formation consequently illustrates how such an environment can succeed in forming dust. Once enough material has reached large distances, at high enough densities, the grains coalesce. □

Received 15 March; accepted 25 April 1994.

1. Gehrz, R. *A. Rev. Astr. Astrophys.* **26,** 377–412 (1988).
2. Payne-Gaposchkin, C. *The Galactic Novae* (North-Holland, Amsterdam, 1957).
3. Zellner, B. *Astr. J.* **76,** 651–654 (1971).
4. Ney, E. P. & Hattfield, B. F. *Astrophys. J.* **219,** L111–L115 (1978).
5. Gehrz, R. D., Grasdalen, G. L., Hackwell, B. F. & Ney, E. P. *Astrophys. J.* **237,** 855–865 (1980).
6. Kanatsu, K. *IAU Circ. No.* 5902 (1994).
7. Savage, B. & Mathis, J. *A. Rev. Astr. Astrophys.* **17,** 73–111 (1979).
8. Mathis, J. *A. Rev. Astr. Astrophys.* **28,** 37–70 (1990).
9. Spitzer, L. *Physics of the Interstellar Medium* (Wiley, New York, 1978).
10. Shore, S. N., Sonneborn, G., Starrfield, S., Gonzalez-Riestra, R. & Polidan, R. *Astrophys. J.* **421,** 344–349 (1994).
11. Garnavich, P. *IAU Circ. No.* 5941 (1994).
12. Kidger, M., Devaney, N., Sahu, K. & Lopez, S. *IAU Circ. No.* 5936 (1994).
13. Scott, A. D., Evans, A. & Geballe, T. *IAU Circ. No.* 5922 (1994).
14. Hauschildt, P. H., Starrfield, S., Shore, S. N., Sonneborn, G. & Allard, F. *Astr. J.* (in the press).
15. Starrfield, S. in *The Classical Novae* (eds Bode, A. & Evans, N.) 127–137 (Wiley-Halstead, New York, 1989).
16. Shore, S. N., Starrfield, S., Hauschildt, P. H., Sonneborn, G. & Gonzalez-Riestra, R. *IAU Circ. No.* 5925 (1994).
17. Scott, A. D., Evans, A., Rawlings, S. & Eales, S. *IAU Circ. No.* 5916 (1994).
18. Humphreys, R. M. in *Massive Stars: Their Lives in the Interstellar Medium* (eds Cassinelli, J. & Churchwell, E. S.) 179–185 (Astr. Soc. of Pacific, Conf. No. 35, San Francisco, 1993).
19. Altner, B. & Shore, S. N. *Bull. Am. Astr. Soc.* **22,** 1258 (1991).
20. Nota, A. *et al. Astrophys. J.* **398,** 621 (1992).
21. Shore, S. N. in *Massive Stars: Their Lives in the Interstellar Medium* (eds Cassinelli, J. & Churchwell, E. S. 186–198 (Astr. Soc. of Pacific Conf. No. 35, San Francisco, 1993).
22. Davidson, K. *Astrophys. J.* **317,** 760–764 (1987).

ACKNOWLEDGEMENTS. We thank C.-C. Wu for IUE observing time, and C. Proffitt and L. Rawley for their assistance. We also thank the IUE observatory staff, and the GSFC and Vilspa schedulers for permitting us to disrupt the observatory operations. S. Lesher assisted with some of the observations. We also thank Y. Takenaka for his regular updates on the optical photometry, the amateur astronomers whose work has made observations of this nova possible, and R. D. Gehrz for his valuable comments as referee. S.N.S., S.S., R.G.-R. and G.S. are Guest Observers, International Ultraviolet Explorer Satellite.

Optical measurements of the superconducting gap in single-crystal K_3C_{60} and Rb_3C_{60}

L. Degiorgi*, G. Briceno†, M. S. Fuhrer†, A. Zettl† & P. Wachter*

* Laboratorium für Festkörperphysik ETH-Zürich, CH-8093 Zürich, Switzerland
† Department of Physics, University of California at Berkeley, Berkeley, California 94720, USA

THE mechanism of superconductivity in alkali-metal compounds of C_{60} (refs 1, 2) remains controversial. Electron-pairing mechanisms based on electron–phonon coupling involving both low-frequency (intermolecular) vibrations[3] and high-frequency (intramolecular) modes[4,5]—the strong-coupling and weak-coupling cases respectively—have been proposed. These two mechanisms have different associated energy scales, which is reflected in the magnitude of the superconducting energy gap. Measurements of the gap for these compounds have been reported previously for powder samples[6–8], but are somewhat discrepant or ambiguous, perhaps owing to grain-size or grain-junction effects. Here we report measurements on large single-crystal samples of K_3C_{60} and Rb_3C_{60} using optical reflectivity. We obtain values for the reduced gap ratio, $2\Delta/k_BT_c$, of 3.44 and 3.45 respectively, consistent with predictions for a mechanism based on standard Bardeen-Cooper-Schrieffer (BCS) electron–phonon coupling to intramolecular modes.

High-quality single crystals of K_3C_{60} and Rb_3C_{60} were prepared by doping vapour-transport-grown C_{60} crystals with alkali metals. The synthesis follows a method similar to that described previously[9,10]. The crystals had a superconducting transition temperature T_c of 20.3 and 30.5 K (that is, where the resistivity $\rho(T_c)=0$ (refs 9, 10)), and had large and shiny surfaces with dimensions 1.5×2 mm and 2×2 mm for K_3C_{60} and Rb_3C_{60}, respectively.

Reflectivity measurements ($R(\nu)$) were performed between 2 meV and 6 eV as a function of temperature using three different spectrometers, with overlapping frequency ranges as described in previous work[8]. The absolute accuracy of the measurement is ~0.8%, whereas the relative accuracy (important for the temperature dependence of $R(\nu)$) is better than 0.3%.

The reflectivity of Rb_3C_{60} in the normal state is displayed in Fig. 1 (results for K_3C_{60} are similar). Besides the overall metallic behaviour (see inset and ref. 8), we recognize in the mid-infrared frequency range two well defined absorptions at 0.07 and 0.17 eV, which are ascribed to the infrared-active T_{1u} phonon modes[11,12]. These modes were missing in our previous investigation of the pressed-pellet specimens (probably because of the large surface scattering due to the grains)[8]. Their appearance and the fair agreement with the expected frequency of these modes for this alkali-metal doping level (that is, A_xC_{60} with $x=3$)[11,12] are evidence for the very good quality of the samples and the outstanding resolution of these new optical measurements.

Figure 2 presents the reflectivity spectra in the far-infrared of K_3C_{60} and Rb_3C_{60} single crystals. It is clearly seen that below 0.014 eV, $R(\nu)$ is enhanced and the onset of this BCS-like enhancement is coincident with T_c. At the lowest temperature (~6 K) the reflectivity is, within experimental error, 100% below a threshold frequency of ~6 and 9 meV for K_3C_{60} and Rb_3C_{60}, respectively. By performing Kramers–Kronig transformations[8], we obtain the optical conductivity $\sigma_1(\nu)$, which is displayed in Fig. 3 at several temperatures. The optical conductivity at 6 K is zero up to the threshold frequencies indicated above, which we ascribe to the optical identification of the superconducting gap. These values correspond to a reduced gap ratio of $2\Delta/k_BT_c=3.44$ and 3.45 for K_3C_{60} and Rb_3C_{60}, respectively, which suggests a weak coupling BCS limit. Our earlier measurements[8] on a pressed pellet hinted at this conclusion; but scattering due to grain-size effects may play an important role in polycrystalline samples, reducing or partially smearing out the intrinsic gap value.

The normal-state properties (spectra above T_c in Fig. 3) deviate considerably from the simple Drude behaviour expected for conventional metals (that is, $\sigma_1(\nu)$ should be constant in the frequency range of Fig. 3), as discussed in ref. 8. This is due to a broad mid-infrared absorption at ~60 meV, which produces a shallow minimum in $\sigma_1(\nu)$ around 12 meV. The presence of such a mid-infrared absorption might lead to another explanation of the data: that the behaviour of $R(\nu)$ below T_c is due to a type of plasma-edge effect[13]. Both the coincidence with T_c of the onset of the temperature dependence of $R(\nu)$, and particularly the absence of any zero crossing of the real part of the dielectric function $\varepsilon_1(\nu)$ (which would define the screened plasma frequency)[13] in the far-infrared frequency range, clearly rule out this explanation.

The experimental electrodynamic response is in a fairly good agreement with the Mattis–Bardeen calculation within the BCS framework[14] or, in a more sophisticated way, with the predictions of the standard Eliashberg theory, as discussed previously for polycrystalline specimens[8]. Within the Eliashberg formalism, one considers a realistic phonon spectrum and directly singles out those phonon modes that are relevant for superconductivity. This approach reduces to the weak coupling BCS Mattis–Bardeen calculation in the limit of the average phonon frequency being much greater than T_c, but impurity scattering effects can also be incorporated. We found that the self-consistent Eliashberg calculation within a phonon model spectrum dominated by high-frequency intramolecular modes gives a reduced gap ratio of ~3.5 and moreover reproduces perfectly the experimental dynamical conductivity[8]. On the contrary, an important disagreement is found when low-energy

© 1994 Nature Publishing Group

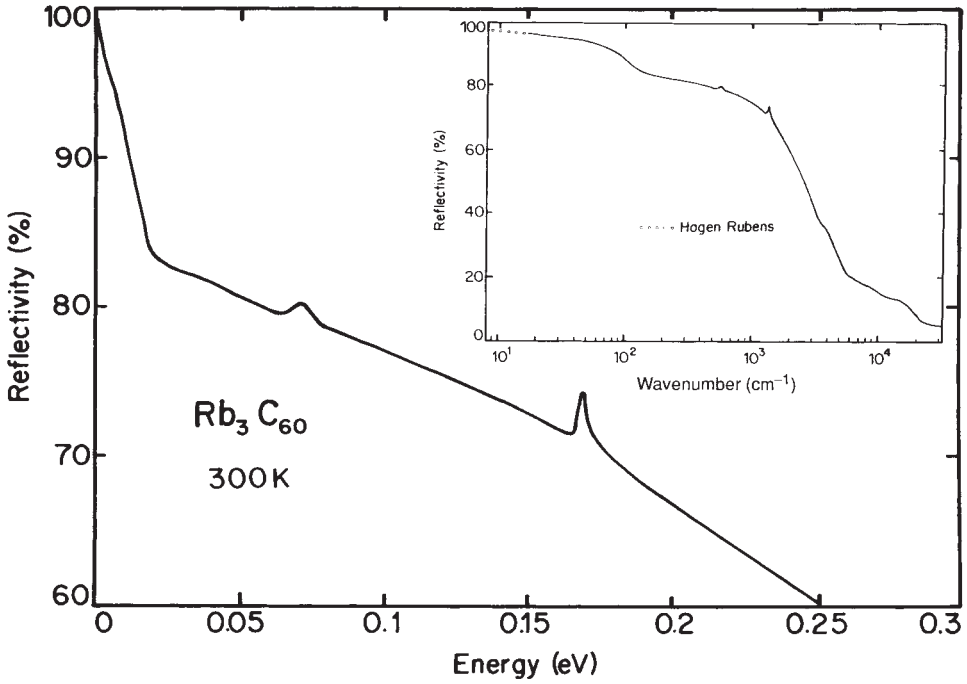

FIG. 1 Normal state reflectivity spectrum of Rb_3C_{60} in the mid-infrared frequency range. The inset displays the whole spectrum (note the logarithmic scale). The Hagen Rubens extrapolation of the reflectivity data to zero frequency corresponds to the expression $R(\nu) = 1 - 2(\nu/\sigma_0)^{1/2}$, where σ_0 is the d.c.-conductivity.

phonon modes are considered; then, $2\Delta/k_BT_c$ turns out to be of the order of 5. This is consistent with the conclusions of other experiments. The specific-heat isotope effect and the normal-state susceptibility investigations[15,16], the pressure and temperature dependence of the nuclear spin lattice relaxation[17], and the muon spin relaxation (μSR) experiments[7], are also strongly indicative that the relevant excitation for the pairing mechanism is related to high-frequency intramolecular phonon modes, thus being consistent with a BCS weak-coupling limit.

Although tunnelling measurements[6] show a BCS-like density of states in the superconducting phase, they indicate a reduced gap ratio ($2\Delta/k_BT_c$) larger than 5, implying a strong-coupling limit. On the other hand, a recent μSR experiment shows a reduced Hebel–Slichter peak, compared to the BCS prediction[7]. This latter result might indicate a significant broadening in the density of states $D_s(E)$ in the superconducting phase. However, it remains to be seen whether this discrepancy of the gap ratio could be traced to such a broading of $D_s(E)$.

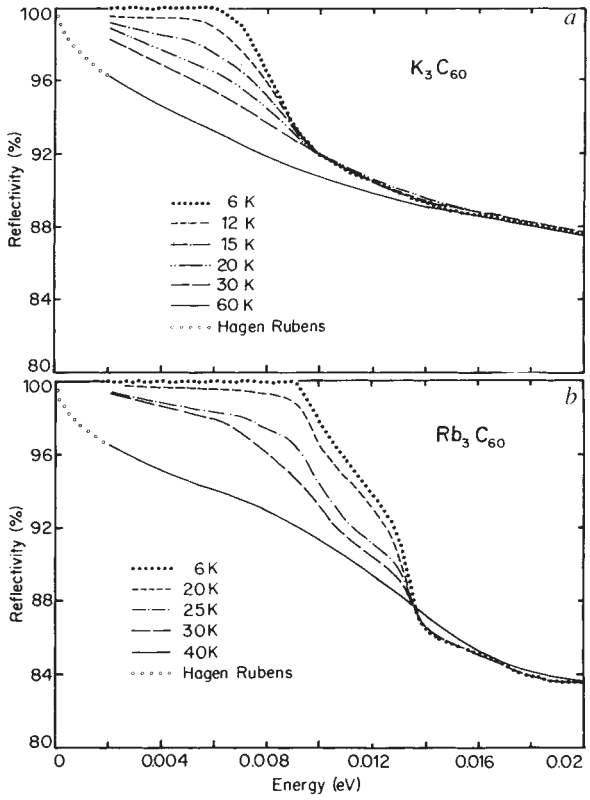

FIG. 2 Far-infrared reflectivity spectra above and below T_c of K_3C_{60} (*a*) and Rb_3C_{60} (*b*).

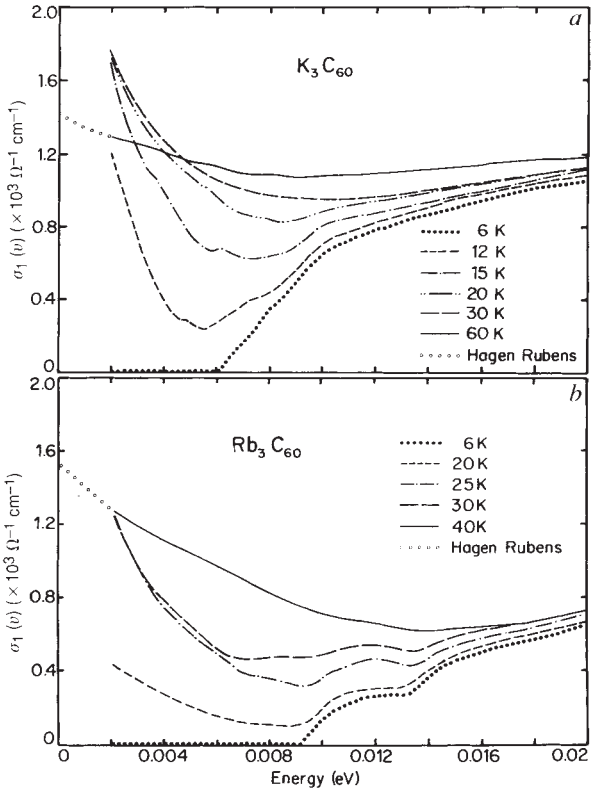

FIG. 3 Optical conductivity in the far-infrared above and below T_c of K_3C_{60} (*a*) and Rb_3C_{60} (*b*).

© 1994 Nature Publishing Group

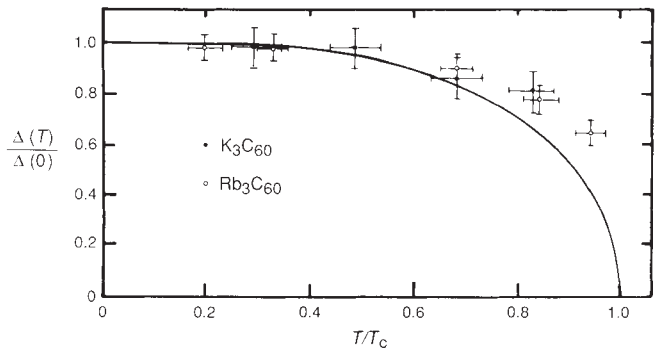

FIG. 4 Temperature dependence of the experimentally obtained superconducting gap (renormalized to $\Delta(0) = 1.76k_BT_c$), compared with the weak-coupling limit of the BCS theory (solid line). The empty and filled circles refer to Rb_3C_{60} and K_3C_{60}, respectively. The error bars correspond to ±1 K and ±0.25 meV.

Figure 3 also displays the temperature dependence of the optical conductivity from the superconducting ground state up to the normal state. First, we note that the K_3C_{60} data (Fig. 3*a*) might be also suggestive of the appearance of the so-called coherence peak at low frequencies (below 3 meV). But because this feature is at the very lower end of our experimentally accessible frequency range, at present we consider this possibility very unlikely. The possibility needs to be investigated, however, by further experiments in the frequency range below the far-infrared. Nevertheless, the overall optical conductivity increases with increasing temperature due to the progressively larger amount of free charge carriers excited across the superconducting gap. The temperature dependence of the superconducting gap can be evaluated either by the maximum of the so-called relative reflectivity given by the ratio R_s/R_n of the reflectivity in the superconducting state over the reflectivity in the normal state, or by fitting the temperature dependence of the experimental ratio σ_{1s}/σ_{1n} with the Mattis–Bardeen BCS calculation[14]. Figure 4 shows the temperature dependence of Δ, normalized to $\Delta(0) = 1.76k_BT_c$, as evaluated from the Mattis–Bardeen approach. While the general trend seems to be suggestive of a BCS-like behaviour, the gap ratio is always enhanced with respect to the BCS prediction as T_c is approached. Previous optical investigations[8,18,19] also indicated an anomalous temperature independence of Δ. Thermal broadening, particularly close to T_c where a realistic determination of Δ is impossible, might be important so that the intrinsic temperature dependence of Δ is beyond the precision of the optical measurement[8]. Moreover, a gap distribution, due to a different T_c (that is, inhomogeneity of the specimens)[18,19] has been also suggested. Such a gap distribution can be, furthermore, the consequence of a gap anisotropy at the Fermi level, so that as the temperature is lowered below the onset of the transition, the regions with large gaps become superconducting first, with regions of smaller gaps following at lower temperatures[18,19]. Alternatively, the temperature dependence of the gap (Fig. 4) might be reminiscent of a fairly broad density of states, as also suggested experimentally by the μSR investigation[7]. All these effects cause the apparent weak temperature dependence of the gap feature when the temperature is raised towards T_c. □

Received 2 March; accepted 29 April 1994.

1. Hebard, A. F. *et al. Nature* **350,** 600–601 (1991).
2. Holczer, K. *et al. Science* **252,** 1154–1157 (1991).
3. Zhang, F. C., Ogata, M. & Rice, T. M., *Phys. Rev. Lett.* **67,** 3452–3455 (1991).
4. Varma, C. M., Zaanen, J. & Raghavachari, K. *Science* **254,** 989–992 (1991).
5. Schluter, M., Lannoo, M., Needels, M., Baraff, G. A. & Tomanek D. *Phys. Rev. Lett.* **68,** 526–529 (1992).
6. Zhang, Z., Chen, C.-C., Kelty, S. P., Dai, H. & Lieber, C.M. *Nature* **353,** 333–335 (1991).
7. Kiefl, R. F. *et al. Phys. Rev. Lett.* **70,** 3987–3990 (1993).
8. Degiorgi, L. *et al.* Phys. Rev. B**49,** 7012–7025 (1994).
9. Xiang, X. D. *et al. Science* **256,** 1190–1191 (1992).
10. Xiang, S. D., Hou, J. G., Crespi, V. H., Zettl, A. & Cohen, M. L. *Nature* **361,** 54–56 (1993).
11. Martin, M. C., Koller, D. & Mihaly, L. *Phys. Rev.* B**47,** 14607–14610 (1993).
12. Iwasa, Y., Yasuda, T., Koda, T. & Koda, S. *Phys. Rev. Lett* **69,** 2284–2287 (1992).
13. Bonn, D. A. *et al. Phys. Rev.* B**35,** 8843–8845 (1987).
14. Mattis, D. C. & Bardeen, J. *Phys. Rev.* **111,** 412–417 (1958).
15. Ramirez, A.P. *et al. Phys. Rev. Lett.* **68,** 1058–1060 (1992).
16. Ramirez, A. P., Rosseinsky, M. J., Murphy, D. W. & Haddon, R. C. *Phys. Rev. Lett.* **69,** 1687–1690 (1992).
17. Quirion, G. *et al. Europhys. Lett.* **21,** 233–238 (1993).
18. Rotter, L. D. *et al. Nature* **355,** 532–534 (1992).
19. Fitzgerald, S. A., Kaplan, S. C., Rosenberg, A., Sievers, A. J. & McMordie, R. A. S. *Phys. Rev.* B**45,** 10165–10168 (1992).

ACKNOWLEDGEMENTS. We thank E. J. Nicol, G. Grüner, M. J. Rice and T. M. Rice for discussion and J. Müller for technical assistance. The research at UCB was supported by the US National Science Foundation and by the Materials Sciences Division of the US Department of Energy. One of us (L.D.) thanks the Swiss National Foundation for Scientific Research for support.

Zeolite-encapsulated Mn(II) complexes as catalysts for selective alkene oxidation

Peter-Paul Knops-Gerrits, Dirk De Vos, Frédéric Thibault-Starzyk & Pierre A. Jacobs*

Centrum voor Oppervlaktechemie en Katalyse,
KU Leuven, Kardinaal Mercierlaan 92, B-3001 Heverlee, Belgium

COMPLEXES of manganese(II) with bipyridine (bpy) have the potential to act as catalysts for oxidation of alkanes and alkenes when the complex is oxidized in acidic conditions[1–6]. But their catalytic activity in solution is limited by their catalase activity[7]—their tendency to decompose H_2O_2. Because of their polynuclear nature such complexes cannot induce epoxidation of alkenes, and other epoxidation catalysts suffer from self-oxidation and side reactions[8–11]. Moreover, all of these homogeneous catalytic processes require phase-transfer conditions. Here we report that, when encapsulated in the supercages of zeolites X and Y, *cis*-$[Mn(bpy)_2]^{2+}$ complexes can catalyse selective epoxidation of alkenes without complications from competing processes such as self-oxidation or catalase activity. Epoxidation of cycloalkenes is followed by acid-catalysed ring-opening, carbon–carbon bond cleavage and formation of alkenedioic acids (Fig. 1). All of the various intermediates in the process can be obtained selectively by controlling the reaction conditions and zeolite acidity. Thus this supramolecular system provides a clean, one-step heterogeneous catalytic route to useful industrial products.

Synthesis of *cis*-manganese(II) bis-2,2′-bipyridyl complex encaged in zeolite NaX and NaY ($[cMn(bpy)_2]^{2+}$-X and $[cMn(bpy)_2]^{2+}$-Y), is performed by a stepwise method based on the synthesis of Fe and Ru tris-bipyridyl-Y complex[12,13], but using the appropriate transition-metal to ligand ratio. MnY (or MnX) zeolite was prepared by ion exchange of NaY (or NaX) with a 2 mM aqueous solution of $Mn(CH_3COO)_2$. The MnY (MnX) zeolite containing 8 Mn^{2+} ions per unit cell (1 Mn^{2+} per supercage) was then washed, filtered and dried at 423 K under a N_2 flow. This material is used as reference in the catalytic experiments. In an inert atmosphere glove-box, 0.4 g of the bpy ligand was added to 2.0 g of the dried MnY (or MnX). The mixture was heated at 363 K for 24 h in a closed system to stimulate complex formation, then Soxhlet-extracted for 24 h with CH_2Cl_2 to remove the unreacted ligand.

Thermo-gravimetric and chemical analysis (CA) performed on $[cMn(bpy)_2]^{2+}$-Y showed that after extraction an average number of 2.02 ± 0.05 bpy per supercage and per Mn^{2+} ion remain in the sample. This ratio corresponds to the proposed stoichiometry of the complex. Chemical analysis and electron spectroscopy for chemical analysis (ESCA) show that bulk- and

* To whom correspondence should be addressed.

© 1994 Nature Publishing Group